

Supplementary information: Correlation between electronic structure and the emergence of superconductivity in $\text{Bi}_{2-x}\text{Sb}_x\text{Te}_{3-y}\text{Se}_y$ ($y \sim 1.2$) studied by x-ray emission spectroscopy and density functional theory

Hitoshi Yamaoka ^{1,*} Harald O. Jeschke ² Huan Li ^{2,†} Tong He ^{2,‡} Naohito Tsujii ³,
Nozomu Hiraoka ⁴ Hirofumi Ishii ⁴ Hidenori Goto ² and Yoshihiro Kubozono ²

¹RIKEN SPring-8 Center, Sayo, Hyogo 679-5148, Japan

²Research Institute for Interdisciplinary Science, Okayama University, Okayama 700-8530, Japan

³International Center for Materials Nanoarchitectonics,

National Institute for Materials Science, Senken 1-2-1, Tsukuba, 305-0047, Japan

⁴National Synchrotron Radiation Research Center, Hsinchu 30076, Taiwan

I. ADDITIONAL XAS SPECTRA

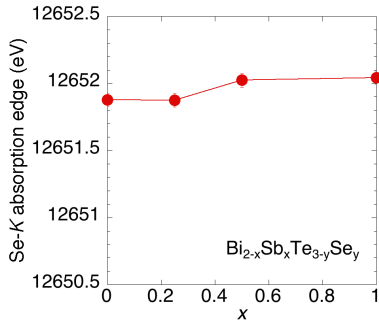


FIG. 1. x dependence of the Se- K absorption edge energy.

Figure 1 shows the x dependence of the Se- K absorption edge energy.

Figure 2 shows the pressure dependence of the PFY-XAS spectra of $\text{Bi}_{2.1}\text{Te}_{1.8}\text{Se}_{1.2}$ at the Se- K and the Bi- L_3 absorption edges. The intensity of the peak A decreased and the width of the peak A also becomes broad with pressure. The Se- K absorption edge shifts to lower incident energy with pressure. Pressure dependence of PFY-XAS spectra of the $x=0$ sample at the Bi- L_3 edge shows that there is an apparent change in the electronic structure at the pressure between 11.16 and 14.31 GPa.

II. PRESSURE DEPENDENCE OF THE d STATES

Figures 3(a) and 3(b) show the pressure dependence of the intensity of the peak $E + F$, corresponding to the Bi

total d empty states. They show no significant pressure dependences within errors.

III. SUPERCONDUCTING T_c AND VOLUME UNDER PRESSURE

TABLE I. Lattice parameters of $\text{Bi}_{2.1}\text{Te}_{1.8}\text{Se}_{1.2}$ in phase I, space group $R\bar{3}m$.

P (GPa)	a (Å)	c (Å)
2.37	4.2226	29.225
4.63	4.18302	28.9
6.58	4.15499	28.532
8.36	4.11888	28.223
9.79	4.0886	28.049
10.94	4.0689	27.961
12.03	4.0587	27.912

Figure 4 shows the pressure dependence of T_c and volume, where the data were taken from the literature [3]. The Sb substitution causes a systematic shift of the phase transition pressures to higher pressures. $\text{Bi}_{2-x}\text{Sb}_x\text{Te}_{3-y}\text{Se}_y$ does not show superconductivity down to 2 K at ambient pressure. [3] Superconductivity appears under pressures on the order of a few GPa. T_c shows a rapid increase at $x = 0$ and 0.5 around the first structural phase transition pressure (P_{s1}). In $\text{Bi}_{1.5}\text{Sb}_{0.5}\text{Te}_{1.68}\text{Se}_{1.32}$, superconductivity was observed

TABLE II. Lattice parameters of $\text{Bi}_{2.1}\text{Te}_{1.8}\text{Se}_{1.2}$ in phase II, space group $C2/m$.

P (GPa)	a (Å)	b (Å)	c (Å)	γ (°)
8.36	14.427	4.0272	17.305	149.577
9.79	14.332	4.0349	17.213	149.398
10.94	14.2343	4.0435	17.047	149.145
12.03	14.1847	4.0337	17.007	149.023
13.30	14.1446	4.0106	16.938	148.949
14.40	14.1049	3.9863	16.879	148.942
15.36	14.0079	3.9443	16.7575	148.711
17.32	13.9956	3.9119	16.7605	148.694

* Corresponding author: yamaoka@spring8.or.jp

† Present address: SusTech Energy Institute for Carbon Neutrality, Department of Mechanical and Energy Engineering, Southern University of Science and Technology, Shenzhen 51805, China

‡ Present address: School of Chemistry & Chemical Engineering, Shaanxi Normal University, Chang'An, Xi'An, Shaanxi 710121, China

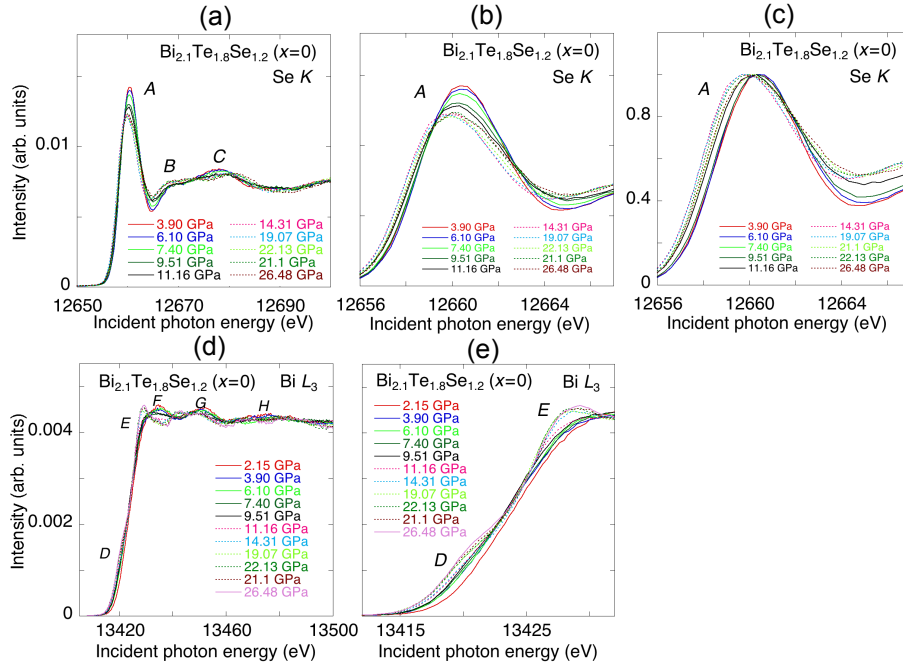


FIG. 2. Absorption spectra of $\text{Bi}_{2.1}\text{Te}_{1.8}\text{Se}_{1.2}$. (a) Pressure dependence of the PFY-XAS spectra at the Se- K absorption edge. (b) Expanded views of the PFY-XAS spectra in (a) around the Se K -absorption edge. (c) Expanded views of the PFY-XAS spectra in (a) around the Se K -absorption edge, where the intensity is normalized to the peak. (d) Pressure dependence of the PFY-XAS spectra at the Bi- L_3 absorption edge. (e) Expanded views of the PFY-XAS spectra in (d) around the Bi- L_3 absorption edge.

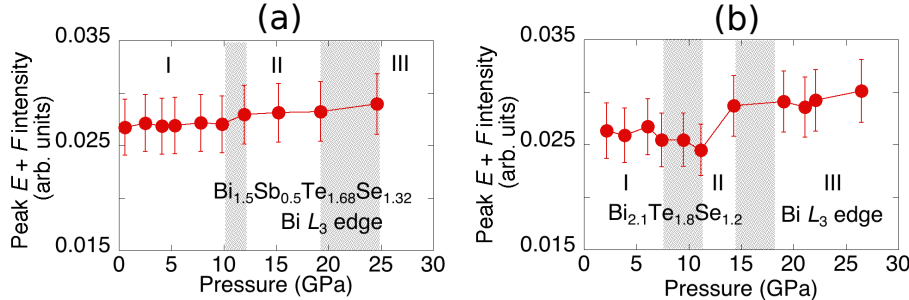


FIG. 3. (a) Pressure dependence of the intensity of the peak $E + F$ for $\text{Bi}_{1.5}\text{Sb}_{0.5}\text{Te}_{1.68}\text{Se}_{1.32}$. (b) Pressure dependence of the intensity of the peak $E + F$ for $\text{Bi}_{2.1}\text{Te}_{1.8}\text{Se}_{1.2}$.

TABLE III. Lattice parameters of $\text{Bi}_{2.1}\text{Te}_{1.8}\text{Se}_{1.2}$ in phase III, space group 9/10-fold $C2/m$.

P (GPa)	a (\AA)	b (\AA)	c (\AA)	γ ($^\circ$)
15.36	15.246	4.9746	6.1086	107.014
17.32	15.2627	4.9815	6.1022	106.895
18.94	15.0492	5.0045	6.1583	106.908
22.49	14.9496	5.0245	6.109	106.476
23.99	14.9086	5.0033	6.098	106.329
26.47	14.8729	4.9907	6.0802	106.271
27.23	14.8429	4.982	6.0709	106.228
28.59	14.824	4.978	6.0626	106.164

mic increase in this pressure range. [4] Cai *et al.* showed that in $\text{Bi}_2\text{Te}_2\text{Se}$ superconductivity appears above 6 GPa of P_{s1} and showed a step-like increase of T_c at 15 GPa of the second phase transition pressure (P_{s2}) [5]. This result does not agree with the one by He *et al.* [3]. In the measurements by He *et al.* the onset temperature of superconductivity is 2.7 GPa in the first phase of $R\bar{3}m$ and below the first phase transition pressure for the $x = 0$ sample.

IV. PRESSURE EVOLUTION OF THE LATTICE

Tables I to III show the lattice parameters determined for the $x = 0$ samples of $\text{Bi}_{2-x}\text{Sb}_x\text{Te}_{3-y}\text{Se}_y$ used in this

above 10.2 GPa and the carrier density showed a logarithmic

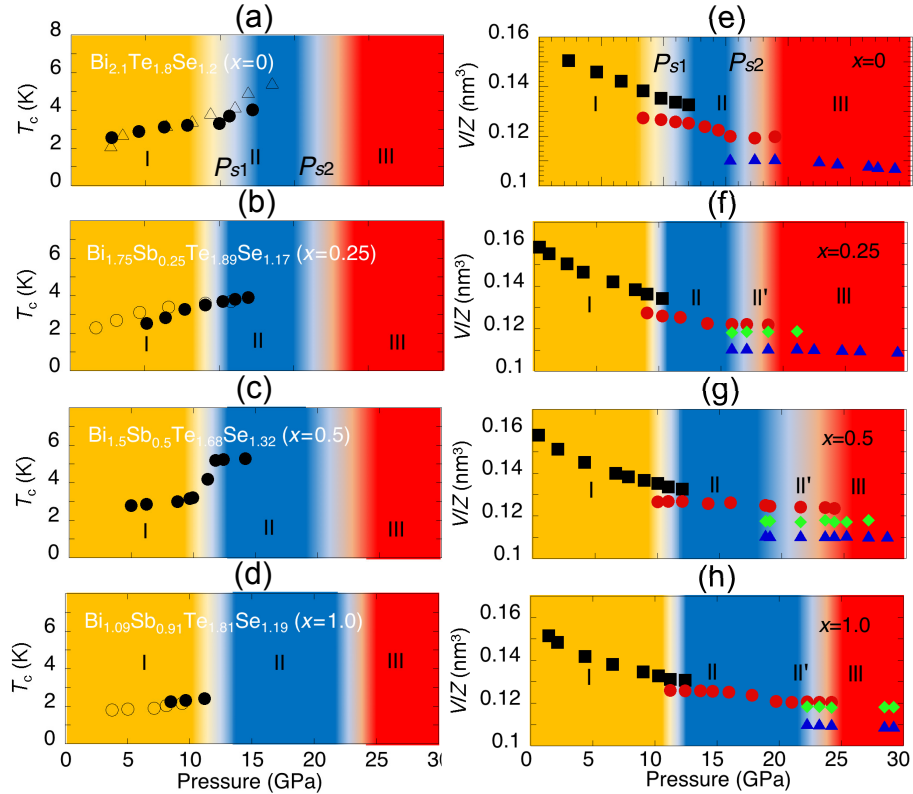


FIG. 4. (a)–(d) Pressure dependence of T_c . [3] (e)–(h) Pressure dependence of volume ($Z = 3$). [3] In (a) & (e) we show the pressures of the first and second structural transitions as P_{s1} and P_{s2} , respectively.

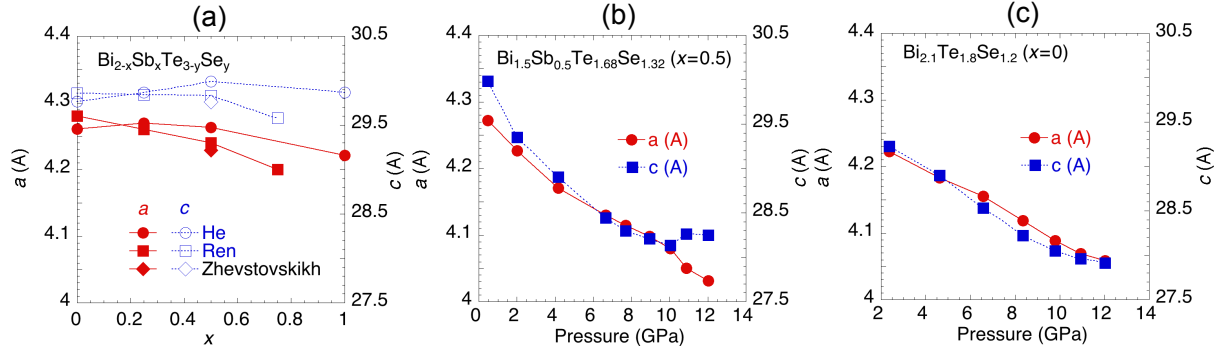


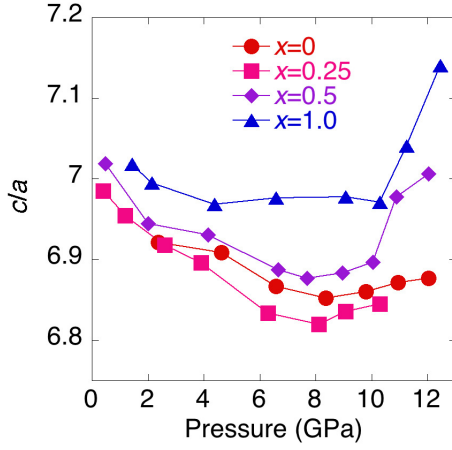
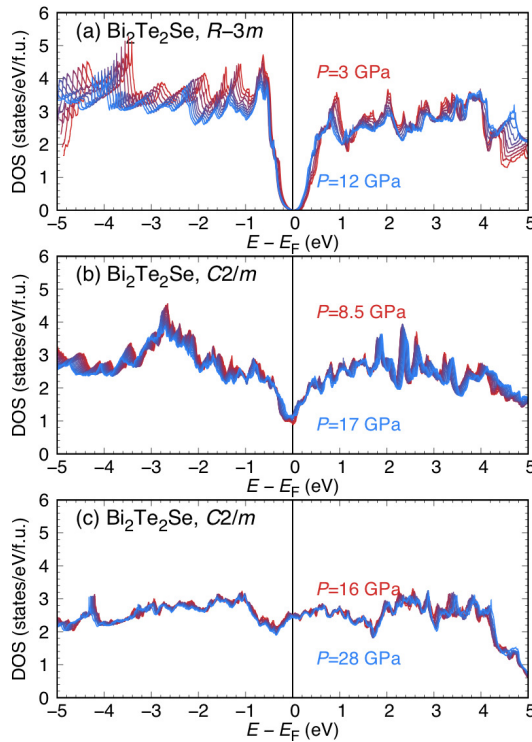
FIG. 5. (a) x dependence of the lattice parameters of $\text{Bi}_{2-x}\text{Sb}_x\text{Te}_{3-y}\text{Se}_y$ ($y \sim 1.2$). (b) Pressure dependence of the lattice parameters of $\text{Bi}_{1.5}\text{Sb}_{0.5}\text{Te}_{1.68}\text{Se}_{1.32}$. (c) Pressure dependence of the lattice parameters of $\text{Bi}_{2.1}\text{Te}_{1.8}\text{Se}_{1.2}$.

work, with the stoichiometry $\text{Bi}_{2.1}\text{Te}_{1.8}\text{Se}_{1.2}$ determined by Rietveld refinement [6]. Tables IV to VII show the lattice parameters determined for the $x = 0.5$ samples of $\text{Bi}_{2-x}\text{Sb}_x\text{Te}_{3-y}\text{Se}_y$ used in this work, with the stoichiometry $\text{Bi}_{1.5}\text{Sb}_{0.5}\text{Te}_{1.68}\text{Se}_{1.32}$ determined by Rietveld refinement [6].

Figure 5 shows (a) the x dependence of the lattice parameters of $\text{Bi}_{2-x}\text{Sb}_x\text{Te}_{3-y}\text{Se}_y$ ($y \sim 1.2$), (b) the pressure dependence of the lattice parameters of $\text{Bi}_{1.5}\text{Sb}_{0.5}\text{Te}_{1.68}\text{Se}_{1.32}$, and (c) the pressure dependence of the lattice parameters of $\text{Bi}_{2.1}\text{Te}_{1.8}\text{Se}_{1.2}$.

In Fig. 6 we show the pressure dependence of the ra-

tio of the lattice constants, c/a . The ratio of c/a takes minimum around 8 GPa. Previously, c/a ratio showed an anomalous minimum at 7 GPa. Anomalous minimum followed by an increase in the c/a ratio is frequently regarded as indicative of electronic topological transition or Lifshitz transition, despite existing debates on the origin.

FIG. 6. Pressure dependence of the ratio c/a .FIG. 7. Evolution of the density of states of $\text{Bi}_2\text{Te}_2\text{Se}$ with pressure.TABLE IV. Lattice parameters of $\text{Bi}_{1.5}\text{Sb}_{0.5}\text{Te}_{1.68}\text{Se}_{1.32}$ in phase I, space group $R\bar{3}m$.

P (GPa)	a (Å)	c (Å)
0.47	4.27184	29.9827
2.01	4.22649	29.35
4.16	4.17049	28.904
6.66	4.12973	28.443
7.69	4.11474	28.298
8.95	4.09797	28.208
10.04	4.07957	28.135
10.88	4.05034	28.263
12.03	4.0315	28.246

TABLE V. Lattice parameters of $\text{Bi}_{1.5}\text{Sb}_{0.5}\text{Te}_{1.68}\text{Se}_{1.32}$ in phase II, space group $C2/m$.

P (GPa)	a (Å)	b (Å)	c (Å)	γ (°)
10.04	14.3915	4.0223	17.2411	149.496
10.88	14.4228	4.035	17.177	149.501
12.03	14.4351	4.0436	17.1172	149.444
14.09	14.4391	4.0198	17.0736	149.442
18.69	14.4986	3.9685	17.1545	149.597
19.06	14.5028	3.9621	17.1819	149.665
21.52	14.5066	3.9651	17.1706	149.702
23.50	14.5067	3.9718	17.1568	149.722
24.22	14.4923	3.9821	17.1198	149.635

TABLE VI. Lattice parameters of $\text{Bi}_{1.5}\text{Sb}_{0.5}\text{Te}_{1.68}\text{Se}_{1.32}$ in phase III, space group $C2/c$.

P (GPa)	a (Å)	b (Å)	c (Å)	γ (°)
18.69	9.6931	6.8481	10.0887	135.411
19.06	9.7343	6.8476	10.1161	135.710
21.52	9.7671	6.8483	10.1241	135.837
23.50	9.7784	6.8495	10.1225	135.924
24.22	9.7666	6.8663	10.0989	135.864
25.23	9.7767	6.8918	10.0616	135.820
26.97	9.7748	6.9226	10.0346	135.754

V. ADDITIONAL ELECTRONIC STRUCTURE CALCULATIONS

In Fig. 7, we show the pressure evolution of the total density of states of $\text{Bi}_2\text{Te}_2\text{Se}$ in the three phases.

Figure 8 shows that density of states at the Fermi level $N(E_F)$ (top) and $s N(E_F)$ (bottom) for $\text{Bi}_2\text{Te}_2\text{Se}$ as function of pressure.

TABLE VII. Lattice parameters of $\text{Bi}_{1.5}\text{Sb}_{0.5}\text{Te}_{1.68}\text{Se}_{1.32}$ in phase IV, space group 9/10-fold $C2/m$.

P (GPa)	a (Å)	b (Å)	c (Å)	γ (°)
18.69	15.255	4.9747	6.1005	106.889
19.06	15.2413	4.9808	6.0974	106.851
21.52	15.2364	4.9816	6.1011	106.553
23.50	15.2313	4.9819	6.0999	106.535
24.22	15.2282	4.98522	6.09271	106.643
25.23	15.2305	4.98747	6.0895	106.57
26.97	15.2305	4.9871	6.08841	106.512

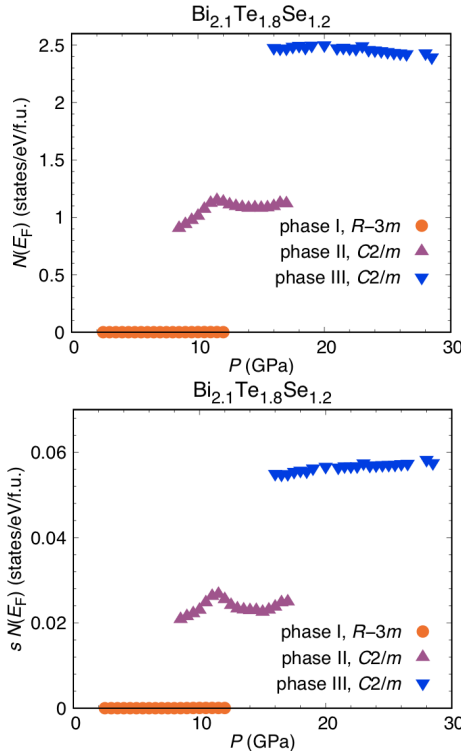


FIG. 8. (Color online) Density of states at the Fermi level $N(E_F)$ (top) and $s N(E_F)$ (bottom) for $\text{Bi}_2\text{Te}_2\text{Se}$ as function of pressure.

- [1] Z. Ren, A. A. Taskin, S. Sasaki, K. Segawa, and Y. Ando, Optimizing $\text{Bi}_{2-x}\text{Sb}_x\text{Te}_{3-y}\text{Se}_y$ solid solutions to approach the intrinsic topological insulator regime, *Phys. Rev. B* **84**, 165311 (2011).
- [2] I. V. Zhevstovskikh, Y. S. Ponosov, S. G. Titova, N. S. Averkiev, V. V. Gudkov, M. N. Sarychev, T. V. Kuznetsova, K. A. Kokh, and O. E. Tereshchenko, Anomalous Behavior of the Elastic and Optical Properties in $\text{Bi}_{1.5}\text{Sb}_{0.5}\text{Te}_{1.8}\text{Se}_{1.2}$ Topological Insulator Induced by Point Defects, *Phys. Stat. Sol. B* **255**, 1800624 (2018).
- [3] T. He, X. Yang, T. Taguchi, T. Ueno, K. Kobayashi, J. Akimitsu, H. Yamaoka, H. Ishii, Y.-F. Liao, H. Ota, H. Goto, R. Eguchi, K. Terashima, T. Yokoya, and Y. Kubozono, Pressure-induced superconductivity in $\text{Bi}_{2-x}\text{Sb}_x\text{Te}_{3-y}\text{Se}_y$, *Phys. Rev. B* **100**, 094525 (2019).
- [4] J. R. Jeffries, N. P. Butch, Y. K. Vohra, and S. T. Weir, Pressure evolution of electrical transport in the 3D topological insulator $(\text{Bi},\text{Sb})_2(\text{Se},\text{Te})_3$, *J. Phys.: Conf. Ser.* **592**, 012124 (2015).
- [5] S. Cai, S. K. Kushwaha, J. Guo, V. A. Sidorov, C. Le, Y. Zhou, H. Wang, G. Lin, X. Li, Y. Li, K. Yang, A. Li, Q. Wu, J. Hu, R. J. Cava, and L. Sun, Universal superconductivity phase diagram for pressurized tetradymite topological insulators, *Phys. Rev. Mater.* **2**, 114203 (2018).
- [6] T. He, Pressure-driven superconductivity in topological insulators, *Ph. D. thesis*, Okayama University (2019).